

## Compressive and tensile strength of aeolian sand stabilized with porcelain polishing waste and hydrated lime

José Daniel Jales Silva<sup>1#</sup> , Olavo Francisco dos Santos Júnior<sup>2</sup> ,  
William de Paiva<sup>3</sup> 

Article

### Keywords

Industrial waste  
Soil stabilization  
Unconfined compressive strength  
Split tensile strength  
Central composite design

### Abstract

The improvement of sandy soils by incorporating new stabilizing agents in a physical and/or chemical process has become the subject of many studies in recent decades. In addition, the use of industrial wastes in this process can bring significant benefits to the environment and savings in natural resources. This work aims to evaluate the implications of incorporating porcelain polishing waste (PPW) and hydrated lime on the mechanical properties of an aeolian dune sand from the city of Natal/RN. Tests of unconfined compressive strength and split tensile strength were performed on compacted soil specimens with different contents of PPW (10%, 20% and 30%), hydrated lime (3%, 5% and 7%) and relative densities (25%, 50% and 75%). To evaluate the effects of each factor, the Response Surface Methodology with Central Composite Design was used. The results have shown that all three factors have a positive effect on the response variables. The highest strengths were obtained in regions combining high values of relative density and PPW content and an optimum lime content was found. An inversely proportional correlation and good fit to the experimental data was obtained between the strength values and the porosity/binder index ( $\eta / B_{iv}$ ). The strength gains were attributed to densification of the soil structure and cementation of the particles by the compounds formed in the reaction between lime and PPW. The results also showed an increase in the strength with curing time, indicating a pozzolanic activity of the mixtures.

## 1. Introduction

Aeolian soils cover large areas in the coastal environment and in regions with arid and semi-arid climates. Urban sprawl and the need for raw materials in the construction industry have led to the use of this type of soil as a foundation layer for buildings and roads or as fill material in embankments and retaining structures (Elipe & López-Querol, 2014). In natural state they have low bearing capacity and a structure susceptible to collapse when wetted (Mohamedzein et al., 2019). Moreover, when saturated and in loose state, are subject to liquefaction under static or cyclic loading, which can cause great damage to materials and human life (Bucci et al., 2018; Bao et al., 2019; Souza Júnior et al., 2020).

The engineering properties of sandy soils, of aeolian origin or formed by other mechanisms, can be significantly improved by a variety of techniques that include densification, reinforcement, drainage or by introducing other materials in a physical, chemical or biological process (Venda Oliveira et al.,

2015; Abbasi & Mahdih, 2018; Venda Oliveira & Rosa, 2020). In the case of chemical stabilization, soil improvement can be achieved by including traditional cementing agents such as Portland cement or newer alternatives such as colloidal silica, bentonite, biopolymers and geopolymers obtained from industrial wastes (Khajeh et al., 2020; Vranna & Tika, 2021; Venda Oliveira & Cabral, 2021; Sharma et al., 2021).

The geotechnical behavior of cemented soils has been studied for decades (Saxena & Lastrico, 1978; Clough et al., 1981; Schnaid et al., 2001; Rios et al., 2014; Vranna & Tika, 2020; Moon et al., 2020). Cementation changes the soil microstructure and hydration products are concentrated at contact points or may also fill part of the voids. In more granular soils the formation of strong bonds at the contact points between the particles increases the strength and stiffness of the structure, with the degree of cementation being directly proportional to the density and number of contacts and inversely proportional to the pore size (Baldovino et al., 2020a). Vranna & Tika (2020) found that even small amounts

<sup>#</sup>Corresponding author. E-mail address: josedanieljales@gmail.com

<sup>1</sup>Universidade Federal de Campina Grande, Unidade Acadêmica de Engenharia Civil, Campina Grande, PB, Brasil.

<sup>2</sup>Universidade Federal do Rio Grande do Norte, Departamento de Engenharia Civil, Natal, RN, Brasil.

<sup>3</sup>Universidade Estadual da Paraíba, Departamento de Engenharia Sanitária e Ambiental, Campina Grande, PB, Brasil.

Submitted on February 20, 2022; Final Acceptance on October 26, 2022; Discussion open until May 31, 2023.

<https://doi.org/10.28927/SR.2023.002322>



This is an Open Access article distributed under the terms of the Creative Commons Attribution License, which permits unrestricted use, distribution, and reproduction in any medium, provided the original work is properly cited.

of cement can optimize the compressive and tensile strength as well as liquefaction resistance of sandy soils by forming bonds between the particles.

On the other hand, alternative materials to Portland cement are being proposed due to the high costs and large environmental impacts associated with the production of this compound (Sharma & Sivapullaiah, 2016; Andrew, 2018). The use of domestic or industrial waste, previously destined for landfills only for containment purposes, helps in the creation of more sustainable and less costly processes and in the conservation of natural resources (Jayanthi & Singh, 2016; Latifi et al., 2018).

Fly ash (Åhnberg, 2006; Mahvash et al., 2018; Simatupang et al., 2020), glass powder (Consoli et al., 2021), nanomaterials (Correia et al., 2021) and biomass waste, especially rice husk ash (Consoli et al., 2019a), have already been effectively used for soil stabilization in mixtures with cement, lime, or by means of the geopolymerization technique, allowing gains in strength, stiffness, and durability. The analysis and prediction of the strength of chemically stabilized soils depends on several factors and has become essential for the use of these materials in engineering applications (Horpibulsuk et al., 2003; Zhang et al., 2013; Correia et al., 2019, 2020).

In the case of pozzolan and lime mixtures, the compressive and tensile strength of the samples can be correlated with the porosity ( $\eta$ ) and the volumetric binder content ( $B_{iv}$ ) using the parameter ( $\eta / B_{iv}$ ), which is the ratio between the volume of binder and the total volume of the sample (Consoli et al., 2018). Several authors have verified the effectiveness of using these parameters for normalizing compressive and tensile strength data (Baldovino et al., 2020b; Consoli et al., 2020a, 2021).

During the manufacturing of porcelain tiles, one of the stages is the polishing of the pieces, responsible for improving the finishing of the product. During this process, which occurs in the presence of water, the residue, generated as a result of the detachment of particles from the tile and the abrasive material, is discarded and is called porcelain polishing waste (PPW). It is estimated that about 100 g of PPW is generated for each m<sup>2</sup> of porcelain tile manufactured (Jacoby & Pelisser, 2015).

This waste, usually discarded in landfills, has a high daily production, requires large storage areas in the industries and can be a source of soil and groundwater contamination, or even be carried by winds affecting the local vegetation (Breitenbach, 2013). Brazil, for example, considered the third largest producer of ceramic pieces in the world, produced 871.9 million m<sup>2</sup> of ceramic tile in 2018 (Anfacer, 2019), and generates about 60,000 tons of PPW per year (De Matos et al., 2018a).

The composition of PPW includes elements present in the ceramic and may also have elements of the abrasive material used in polishing the pieces. Thus, its chemical analysis results in large quantities of silica and alumina.

Magnesium and other fluxing oxides found in porcelain tiles can also be present (Medeiros et al., 2021). Specific tests such as electrical conductivity and calcium hydroxide consumption (Medeiros et al., 2021) or the analysis of cementitious materials with PPW incorporation using mechanical strength tests and thermogravimetry (Jacoby & Pelisser, 2015; De Matos et al., 2018b) confirmed the existence of pozzolanic activity of this material. The incorporation of the residue resulted in an optimization of the hydration reactions of the compounds, allowing gains in strength and durability, and thus constituting a potential candidate for use in soil improvement in mixtures with lime and cement.

However, while several studies have already evaluated the use of this material in the production of cements (Andreola et al., 2010; Jacoby & Pelisser, 2015; De Matos et al., 2020), mortars (Jacoby & Pelisser, 2015; Sánchez de Rojas et al., 2018; Li et al., 2019, 2020) and concretes (De Matos et al., 2018a, b; Medeiros et al., 2021), no research was found evaluating its use in soil improvement processes, thus constituting the main gap that this work aims to address.

In this context, this research aims to use mechanical tests to study the incorporation of porcelain polishing waste and hydrated lime to improve a sandy aeolian soil from a coastal dune located in the city of Natal/RN. Fontoura et al. (2021) investigated the influence of cement content and molding moisture on the mechanical behavior of this soil and obtained an increase in unconfined compressive strength with increasing cement content.

## 2. Materials and methods

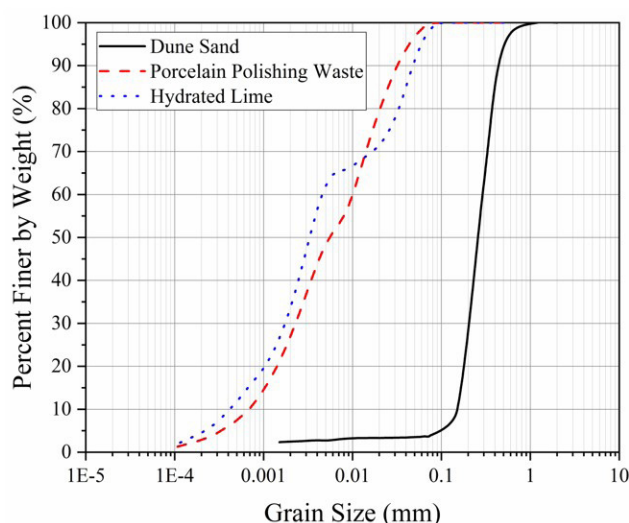
### 2.1 Materials

In this research, dune sand, hydrated lime and a residue from the porcelain tile polishing process were the three materials used. The soil is a quartz sand from sedimentary deposits that form dunes in the coastal region of Natal in Rio Grande do Norte. Figure 1 shows the grain size distribution curve of the sand, while Table 1 presents its physical properties. The material has angular to sub-angular grains and a uniform grading composed of 96.23% particles in the sand fraction (0.06 - 2.00 mm), approximately 70% medium sand, and fines content below 5%, being classified as a poorly graded sand (SP) by the Unified Soil Classification System.

Porcelain polishing waste was obtained from an industry that produces ceramic tiles in the state of Paraíba, Brazil. This waste is generated in the porcelain tile polishing operation with an abrasive material and in the presence of large amounts of water. The material used in this research was the solids resulting from the dewatering of the effluent in a filter press and which is stored in large piles outdoors. Around 200 kg of material was collected in different piles stored at a maximum time of one week, providing greater homogeneity given the variations in the production line.

**Table 1.** Physical properties of dune sand.

Properties	Symbol	Value
Specific gravity (-)	$G_s$	2.66
Mean diameter (mm)	$d_{50}$	0.265
Effective diameter (mm)	$d_{10}$	0.151
Coefficient of uniformity (-)	$C_u$	1.94
Coefficient of curvature (-)	$C_c$	0.98
Maximum void ratio (-)	$e_{ii}$	0.84
Minimum void ratio (-)	$e_{\bar{u}}$	0.60

**Figure 1.** Grain size distribution curves of the materials used in this research.

The collected material was initially homogenized and dried at a temperature of approximately 100 °C for 24 h. The dry material was manually crushed, passed through a sieve with 0.42 mm mesh and then subjected to characterization tests. Figure 1 shows the particle size distribution of PPW that was obtained by laser diffraction granulometer.

The material is composed of 26.93% of particles with dimensions equivalent to clays (< 0.002 mm), 71.61% in the range of silts (0.002 - 0.06 mm) and only 1.46% of particles in the range of fine sands (0.06 - 0.2 mm). In addition, it has 99.74% of fine particles with size below 75 µm, an average diameter ( $d_{50}$ ) of 0.0055 mm and an effective diameter ( $d_{10}$ ) of 0.00068 mm. It presented liquid limit, plastic limit and plasticity index equal to 31%, 27% and 4%, respectively, being classified as a low plastic material. The specific gravity obtained was 2.55. Regarding the chemical composition, PPW presented as main components silica (67.48%) and aluminum (17.91%) that plus iron amount to 86.4%, allowing the material to be classified as a class N pozzolan by ABNT NBR 12653 (ABNT, 2014). The compounds calcium, sodium, magnesium and potassium were also present in smaller amounts.

The main crystalline phases identified were quartz, albite, mullite and silicon carbide, with the first three probably derived from the porcelain paste and the last one from the abrasive material used. The morphology of PPW particles is composed of rough and angular particles of irregular shapes. The consumption of 394 mg of calcium oxide per gram of PPW measured by the Modified Chapelle method was higher than the 330 mg/g limit proposed by Raverdy (Hoppe Filho et al., 2017) confirming the pozzolanic activity of this material. CH-I high purity hydrated lime was used as a source of reactive calcium, this material has a specific gravity of 2.30.

## 2.2 Methods

The variables controlled for the produced samples were relative density ( $RD$ ), lime content ( $L$ ) and PPW content ( $P$ ). To define the levels of each variable and optimize the experimental program the Response Surface Methodology with Central Composite Rotatable Design (CCRD) was used. This technique allows an optimization in the combinations between the various analyzed factors, reducing the necessary amount of samples to be produced (Atkinson & Donev, 1992). The number of experiments is defined based on Equation 1, where  $k$  is the number of factors and  $CP$  the number of central points.

$$n = 2^k + CP + 2 \times k \quad (1)$$

Thus, for 3 factors or independent variables, 15 experiments are obtained, being 8 factorial points (FP), 6 axial points (AP) and 1 central point (CP). All experiments were performed in triplicate. For this research, the PPW content was defined as a replacement for sand and the lime content was defined as an addition to the sand plus PPW mixture.

In order to evaluate the influence of low to high contents of PPW incorporation, 10%, 20%, and 30% were chosen as levels for this variable. In the case of lime, the Initial Lime Consumption method proposed by Rogers et al. (1997) was applied to determine the minimum amount of hydrated lime necessary to reach a pH sufficient to induce pozzolanic reactions in the mixture. The results showed that for the maximum PPW content incorporated the minimum lime content is 3%. Thus, considering the work of other researchers in the area of pozzolan-lime mixtures (Abbasi & Mahdiah, 2018; Consoli et al., 2019b, 2021), contents of 3%, 5% and 7% were adopted. As for the relative density, the aim was to evaluate mixtures in the loose, medium dense and dense states, adopting values of 25%, 50% and 75%, respectively.

The independent variables and the proposed levels with real and coded values for the CCRD are shown in Table 2, while the design matrix of the experiments is shown in Table 3. For each composition, maximum and minimum void ratios tests were performed, whose results are shown in Table 4. The specific gravity of each mixture ( $G_s$ ) is a

function of the contents ( $S, L, P$ ) and densities ( $\rho_S, \rho_L, \rho_P$ ) of each material and the equation for its calculation is derived below (Equations 2 and 3), where  $M_S, M_L$  and  $M_P$  and  $V_S, V_L$  and  $V_P$  are the mass and volume of sand, lime and PPW particles, respectively.  $M_d$  is the total dry mass of the mixture and  $\rho_w$  the density of water.

$$G_s = \frac{M_{solids}}{(V_{solids})\rho_w} = \frac{M_S + M_L + M_P}{(V_S + V_L + V_P)\rho_w} = \frac{\frac{M_d}{1+L}(S+L+P)}{\frac{M_d}{1+L}\left(\frac{S}{\rho_S} + \frac{L}{\rho_L} + \frac{P}{\rho_P}\right)\rho_w} \quad (2)$$

$$G_s = \frac{S+L+P}{\left(\frac{S}{\rho_S} + \frac{L}{\rho_L} + \frac{P}{\rho_P}\right)\rho_w} \quad (3)$$

The experimental data were fitted to a second order polynomial equation  $Y$  (quadratic model), similar to Equation 4. Where,  $X_{(1,2,3)}$  are the independent variables and  $\beta_0, \beta_{(1,2,3)}, \beta_{(11,22,33)}$  and  $\beta_{(12,13,23)}$  are the regression coefficients for, respectively, the intercept, linear and quadratic behavior and interaction between the factors.

$$Y = \beta_0 + \beta_1 X_1 + \beta_2 X_2 + \beta_3 X_3 + \beta_{11} X_1^2 + \beta_{22} X_2^2 + \beta_{33} X_3^2 + \beta_{12} X_1 X_2 + \beta_{13} X_1 X_3 + \beta_{23} X_2 X_3 \quad (4)$$

**Table 2.** Independent variables and levels used in the CCRD.

Factors	Levels				
	-1.68	-1	0	+1	+1.68
Relative density (%)	7.96	25	50	75	92.04
Lime content (%)	1.64	3	5	7	8.36
PPW content (%)	3.18	10	20	30	36.82

In order to validate the statistical models obtained, additional tests in triplicate for unconfined compressive strength and tensile strength were performed under two new conditions (40% RD, 4% lime, 25% PPW and 60% RD, 6% lime, 15% PPW) on samples at 28 days of curing and the results were compared with the predicted values.

**Table 3.** CCRD matrix for compressive and tensile strength tests.

Mixtures	Real value (Coded value)		
	Relative density	Lime content	PPW content
FP-1	25% (-1)	3% (-1)	10% (-1)
FP-2	25% (-1)	3% (-1)	30% (+1)
FP-3	25% (-1)	7% (+1)	10% (-1)
FP-4	25% (-1)	7% (+1)	30% (+1)
FP-5	75% (+1)	3% (-1)	10% (-1)
FP-6	75% (+1)	3% (-1)	30% (+1)
FP-7	75% (+1)	7% (+1)	10% (-1)
FP-8	75% (+1)	7% (+1)	30% (+1)
AP-1	7.96% (-1.68)	5% (0)	20% (0)
AP-2	92.04% (+1.68)	5% (0)	20% (0)
AP-3	50% (0)	1.64% (-1.68)	20% (0)
AP-4	50% (0)	8.36% (+1.68)	20% (0)
AP-5	50% (0)	5% (0)	3.18% (-1.68)
AP-6	50% (0)	5% (0)	36.82% (+1.68)
CP	50% (0)	5% (0)	20% (0)

**Table 4.** Physical properties of each composition.

Contents		Properties				
Lime	PPW	$\gamma_{d_{max}}$ (kN/m <sup>3</sup> )	$\gamma_{d_{min}}$ (kN/m <sup>3</sup> )	$e_{max}$	$e_{min}$	$G_s$
3%	10%	17.0	14.4	0.84	0.55	2.64
3%	30%	17.1	12.7	1.06	0.53	2.62
7%	10%	16.6	14.0	0.88	0.58	2.62
7%	30%	16.0	12.1	1.15	0.62	2.60
1.64%	20%	16.8	13.7	0.91	0.56	2.63
8.36%	20%	16.4	12.7	1.05	0.59	2.61
5%	3.18%	16.7	14.3	0.84	0.58	2.64
5%	36.82%	15.5	11.6	1.24	0.68	2.60
50%	20%	16.6	13.2	0.99	0.58	2.62

### 2.2.1 Molding and curing of the specimens

For all tests, cylindrical specimens with dimensions of 50 mm in diameter and 100 mm in height were used. Initially, the PPW and the sand in dry condition were mixed manually until a homogeneous appearance was obtained. Then hydrated lime was added and a new homogenization was carried out. Distilled water was added to the final material. The void ratio ( $e$ ) (Equation 5) and total dry mass ( $M_d$ ), whose calculation is derived in Equations 6 and 7, were used to obtain the dry mass of each material used in the mixture (Equations 8 to 10). Where  $\rho_d$  is the dry density of the mixtures and  $V_{total}$  the total volume of the sample.

$$e = e_{\text{initial}} - RD \times (e_{\text{initial}} - e) \quad (5)$$

$$\rho_d = \frac{M_d}{V_{total}} = \frac{M_S + M_L + M_P}{V_{solids} (1 + e)} = \frac{\frac{M_d}{1+L} (S + L + P)}{\frac{M_d}{1+L} \left( \frac{S}{\rho_S} + \frac{L}{\rho_L} + \frac{P}{\rho_P} \right)} \times \frac{1}{(1+e)} \quad (6)$$

$$M_d = \frac{(S + L + P)}{\left( \frac{S}{\rho_S} + \frac{L}{\rho_L} + \frac{P}{\rho_P} \right)} \times \frac{V_{total}}{(1+e)} \quad (7)$$

$$M_S = \frac{M_d}{1+L} \times S \quad (8)$$

$$M_L = \frac{M_d}{1+L} \times L \quad (9)$$

$$M_P = \frac{M_d}{1+L} \times P \quad (10)$$

Since the moisture required by each material is different, the mass of water ( $M_w$ ) was calculated based on Equation 11 by adding 5% in relation to the mass of sand ( $M_S$ ) with a water/binder ratio of 0.32. The binder was taken as the sum of the mass between the PPW ( $M_P$ ) and hydrated lime ( $M_L$ ) and this content was chosen based on previous tests in order to have good workability when molding.

$$M_w = 0.05 \times M_S + 0.32 \times (M_L + M_P) \quad (11)$$

The mixtures were statically compacted using a mechanical loading machine in a tripartite cylindrical mold in four layers of equal mass and height. The compaction energy used in each layer was that sufficient to achieve the desired height and, consequently, the target dry unit weight and relative density. The top of each layer was scarified to improve the adhesion between them. A maximum time of 20 minutes was adopted for the mixing and compaction processes in order

to minimize its influence on particle cementation. Three samples were taken to verify the moisture content.

At the end of molding, the specimens were removed from the mold and then weighed to verify their wet weight with 0.01 g precision. Due to the fragility of the samples, dimensions were measured only on some specimens to obtain an average volume used to calculate the relative density. The maximum tolerances adopted for sample acceptance were  $\pm 0.5\%$  for moisture and  $\pm 2\%$  for relative density.

Then the specimens were placed in a humid chamber for curing at a temperature of  $23 \text{ }^\circ\text{C} \pm 3 \text{ }^\circ\text{C}$  and humidity above 95%. The standard curing time was 28 days, however, for the FP-8 mixture, samples were also analyzed at 7 and 91 days of curing to observe the development of cementation reactions over time.

### 2.2.2 Compressive strength tests

At 27 days of curing, the specimens were immersed for 24 h in a container of water to minimize the effects of suction. They were then removed from the tank and superficially dried with an absorbent cloth. The tests were performed on a hydraulic press with a maximum capacity of 100 kN and a load cell with a capacity of 10 kN and resolution of 0.01 kN. The test followed the prescriptions of ABNT NBR 5739 (ABNT, 2018), similar to ASTM C39 (ASTM, 2021), and was initiated immediately after surface drying at a rate of 1.00 mm/min with the maximum load being obtained for each specimen.

The compressive strength is defined as the ratio between the maximum load and the cross-sectional area of the specimen. As an acceptance criterion for the mechanical tests, it was adopted that the individual strengths of the three specimens could not deviate by more than 10% from the average strength.

### 2.2.3 Split tensile strength tests

To obtain the tensile strength of the specimens, split tensile tests, also known as the indirect tensile test or Brazilian Test, were performed. The same machine was used as for the axial compression tests. The procedure followed the prescriptions of ABNT NBR 7222 (ABNT, 2011), similar to ASTM C496 (ASTM, 2017). The specimen, prepared as in the previous test, was placed between two rectangular pieces of wood with dimensions calculated according to the dimensions of the specimen and diametrically opposite to each other. A compression load was then applied generating a diametrical rupture. The tensile strength ( $q_t$ ) was obtained from Equation 12, which relates the maximum applied force ( $F$ ), the diameter ( $D$ ) and height ( $H$ ) of the specimen.

$$q_t = \frac{2F}{\pi DH} \quad (12)$$

For analysis of the results obtained for the response variables, including generation and fitting of the model, obtaining the response surfaces and analysis of data variance, the Statistica 12.0 software was used.

### 3. Results and discussion

#### 3.1 Statistical analysis

A total of 114 specimens were prepared for the experimental program. Table 5 shows all values of unconfined compressive strength ( $q_u$ ) and split tensile strength ( $q_t$ ) calculated as the average of the strength of three specimens as well as the respective standard deviation for 28 days curing time. The  $q_u$  values obtained ranged from 57.39 kPa to 1561.43 kPa, and the values from 7.13 kPa to 162.48 kPa. This indicates that the variables involved in the design have an influence on the mechanical strength of the soil samples. Similar ranges were obtained by Abbasi & Mahdih (2018), Consoli et al. (2018, 2019b, 2021) in mixtures of soil, pozzolan and lime cured at 28 days.

The data analysis using CCRD allowed the identification of significant factors and their respective coefficients to build the regression model. Since the actual values of relative density vary around the planned values ( $\pm 2\%$ ) due to factors inherent to the molding process and to allow the calculation of the pure error and lack of fit parameters, the planned values were considered for all specimens.

In the case of compressive strength, ignoring the effects of insignificant terms ( $p$ -value  $> 0.05$ ), it was possible to obtain an adjusted regression model with coefficient of determination  $R^2$  value of 0.980, i.e., which explains 98.0% of the variability of the process (only 2.0% of the total variability cannot be explained) that is given in Equation 13.

In addition, the adjusted  $R^2$  of 0.976 was very close to the  $R^2$  actual value, indicating a good fit of the second-order polynomial equation to the experimental data. The result of the analysis of variance (ANOVA) with the fitted model is shown in Table 6. The sum of squares ( $SS$ ), degrees of freedom ( $df$ ), mean square ( $MS$ ) and  $p$ -value are shown. The lack of fit test was used to evaluate the model fit by comparing the pure error with the residual error. The result showed a significant lack of fit, however, the other evaluations such as the coefficient of determination and an analysis of the distribution of residuals showed that the model is able to predict with quality the values of the response variable.

$$q_u = -3.936(RD) - 0.036(RD^2) + 339.488(L) - 27.457(L^2) + 22.052(P) - 0.637(P^2) + 0.865(RD)(P) - 943.208 \quad (13)$$

For the tensile strength only the quadratic term of the PPW content proved to be insignificant and was ignored in the final regression equation. Thus, it was possible to obtain a model with  $R^2$  also equal to 0.980 and adjusted  $R^2$  of 0.976, given in Equation 14. The result of the analysis of variance with the fitted model is shown in Table 7.

$$q_t = -1.551(RD) + 0.005(RD^2) + 24.507(L) - 2.464(L^2) + 0.559(P) + 0.079(RD)(L) + 0.068(RD)(P) + 0.085(L)(P) - 31.841 \quad (14)$$

##### 3.1.1 Model validation

The results of the additional tests for unconfined compressive strength and tensile strength to validate the

**Table 5.** Compressive and tensile strength results for each mixture.

Mixtures	$q_u$ (kPa)	Standard deviation (kPa)	$q_t$ (kPa)	Standard deviation (kPa)	$q_t / q_u$
FP-1	99.30	3.25	8.75	0.32	0.09
FP-2	495.15	16.89	72.65	3.70	0.15
FP-3	288.61	13.43	23.30	0.93	0.08
FP-4	719.66	62.30	74.01	5.11	0.10
FP-5	128.70	9.53	13.73	0.88	0.11
FP-6	1408.08	17.79	125.38	6.09	0.09
FP-7	284.13	8.05	24.05	1.72	0.08
FP-8	1561.43	33.07	162.48	4.96	0.10
AP-1	325.15	22.45	54.52	4.72	0.17
AP-2	1241.88	107.04	113.18	1.57	0.09
AP-3	224.77	6.25	20.83	1.85	0.09
AP-4	849.45	67.47	72.68	5.18	0.09
AP-5	57.39	1.47	7.13	0.13	0.12
AP-6	1277.55	71.74	145.19	5.91	0.11
CP	825.45	66.00	67.64	4.07	0.08

statistical models obtained are presented in this section. The levels of each factor as well as the results found (average values) and percentage error relative to the value predicted by the model are presented in Table 8.

It can be seen that there is a good agreement between the predicted and observed values. All the tests showed a percentage error lower than 10%, indicating that the obtained models can be used to predict with good accuracy the compressive and tensile strengths of this dune sand stabilized with PPW and lime.

### 3.2 Unconfined compressive strength and split tensile strength results

The interaction model of the three independent variables evaluated in the research with the response was obtained to assess the effect of each one on the compressive strength ( $q_u$ ) and tensile strength ( $q_t$ ) of mixtures. With the

**Table 6.** ANOVA for compressive strength quadratic model.

Source	SS	df	MS	p-value
<i>RD</i>	2423320	1	2423320	0.000000
<i>RD</i> <sup>2</sup>	9366	1	9366	0.044625
<i>L</i>	690686	1	690686	0.000000
<i>L</i> <sup>2</sup>	219029	1	219029	0.000000
<i>P</i>	6490356	1	6490356	0.000000
<i>P</i> <sup>2</sup>	73773	1	73773	0.000002
<i>RD</i> × <i>P</i>	1122071	1	1122071	0.000000
Lack of Fit	164859	7	23551	0.000001
Pure Error	63960	30	2132	
Total	11241543	44		

**Table 7.** ANOVA for tensile strength quadratic model.

Source	SS	df	MS	p-value
<i>RD</i>	13246.0	1	13246.02	0.000000
<i>RD</i> <sup>2</sup>	314.6	1	314.61	0.000053
<i>L</i>	4977.8	1	4977.83	0.000000
<i>L</i> <sup>2</sup>	2874.4	1	2874.38	0.000000
<i>P</i>	78262.9	1	78262.94	0.000000
<i>RD</i> × <i>L</i>	372.5	1	372.54	0.000016
<i>RD</i> × <i>P</i>	6881.7	1	6881.74	0.000000
<i>L</i> × <i>P</i>	69.4	1	69.38	0.034724
Lack of Fit	1745.6	6	290.93	0.000000
Pure Error	425.4	30	14.18	
Total	110574.6	44		

**Table 8.** Predicted and observed values for the validation of the statistical models.

Mixtures	Relative density	Lime content	PPW content	$q_u$ (kPa)			$q_t$ (kPa)		
				Predicted	Observed	Error	Predicted	Observed	Error
1	60%	6%	15%	704.07	677.52	-3.77%	57.59	53.88	-6.44%
2	40%	4%	25%	777.69	849.86	9.28%	75.89	79.16	4.31%

model it was possible to generate the response surfaces for the variables studied as well as contour plots allowing the combined influence of the variables on soil strength to be verified. The contour plot provides a two-dimensional representation while the response surface adds a new axis for easy visualization. These graphs allow the evaluation of how each independent variable affects the response at different levels while keeping another independent variable constant. Figure 2 illustrates the response surfaces and contour plots for compressive strength relating it with two independent variables while the third independent variable is held fixed at the center value. The results for tensile strength can be seen in Figure 3.

It can be observed that  $q_u$  and  $q_t$  of the samples present a parabolic increase with the increase in the PPW content for any relative density, however, this increase is more significant and linear at higher values of relative density. These results are in agreement with other works that have evaluated the incorporation of pozzolanic materials and lime for the improvement of soils (Abbasi & Mahdiah, 2018; Consoli et al., 2018, 2021).

In these cases, the strength gain is especially attributed to the cementation of the grains as a result of the pozzolanic reactions between pozzolan and lime, which is amplified with higher silica and aluminum reserves present in the residue. Increases in strength with increasing content of incorporation of pozzolanic wastes were reported by other authors in similar research (Silvani et al., 2019; Simatupang et al., 2020). Lime carbonation can also generate compounds that help in particle cementation. Furthermore, an increase in relative density promotes gains for  $q_u$  and  $q_t$ , especially at high PPW levels. This can be attributed to the reduction in void ratio that increases the number of contacts between the particles and optimizes the load transfer allowing the soil to withstand higher stresses (Vranna & Tika, 2020).

With a reduction in PPW content the effect of relative density is also reduced. At low PPW contents, this material tends to be concentrated in the voids between the larger sand particles that dominate the soil strength mechanism even for denser samples. However, with an increase in the PPW content, the cementation generated can act on the contact between the sand grains and an increase in density amplifies the number of contacts, thus allowing greater impacts on the strength (Chang & Woods, 1992; German, 2014; Vranna & Tika, 2020; Moon et al., 2020; Consoli et al., 2021). The incorporation of smaller particles causes, for the same mass, the number of particles to increase, thus increasing

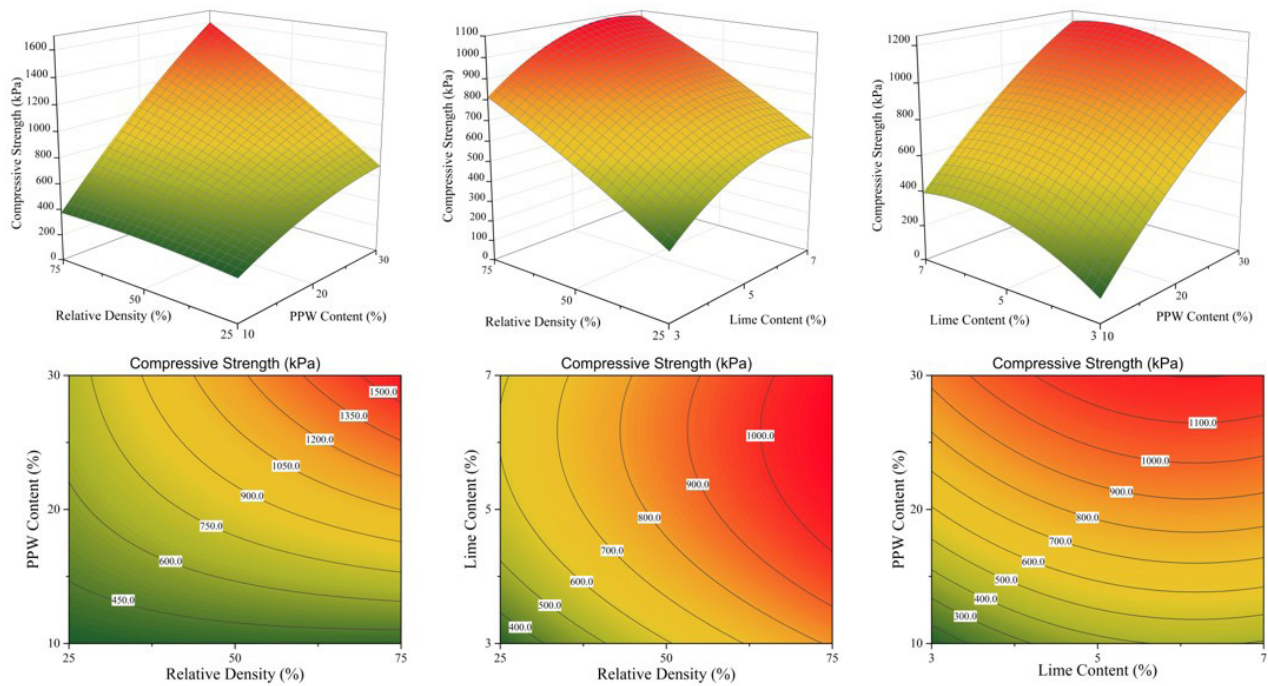


Figure 2. CCRD response surfaces and contour plots for compressive strength.

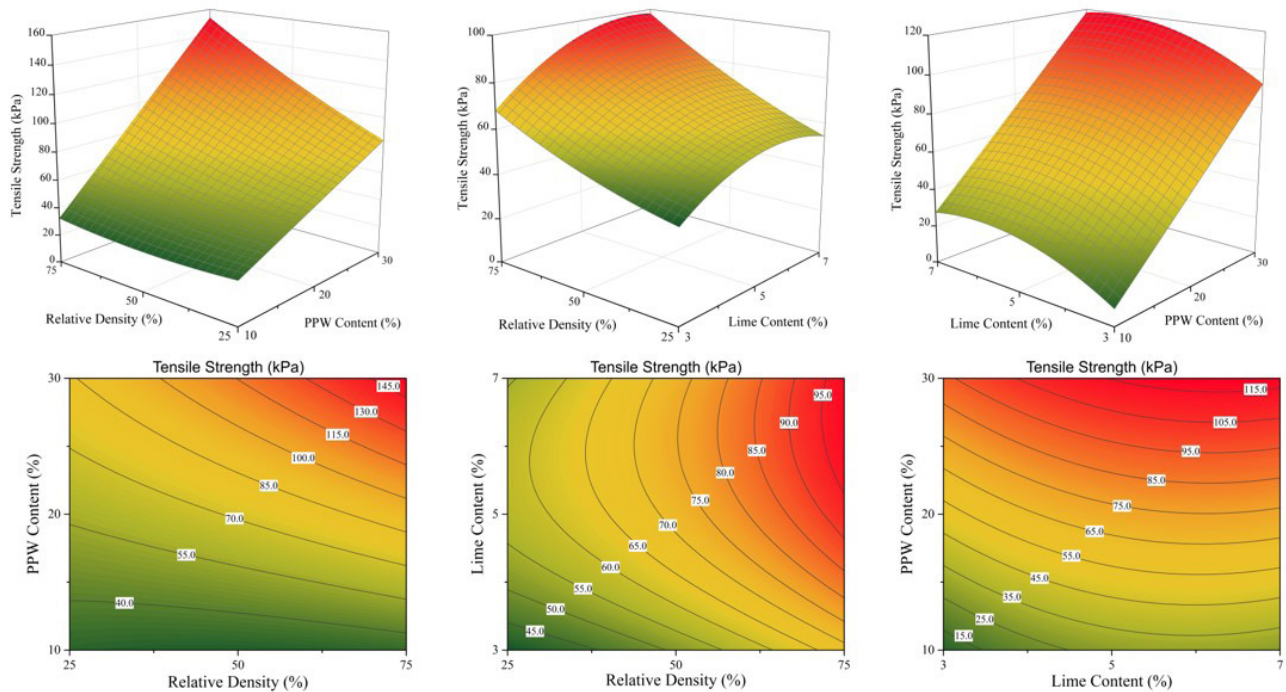


Figure 3. CCRD response surfaces and contour plots for tensile strength.

the number of contacts (Wiącek & Molenda, 2014). Another aspect is that for low saturation levels, hydration products tend to precipitate in regions where the meniscus are formed and that occur in greater numbers with an increase in the number of contacts (Ribeiro et al., 2016). The highest strengths were

found in the region combining high values of PPW content and relative density, indicating that the interaction between them is more important than their isolated effects.

The effect of the lime content on both strengths is given by a parabolic curve with the concavity downward,

indicating that there is an optimum lime content, this behavior is maintained for any relative density. While there is a significant improvement in strength between the samples with 3% and 5% lime, this improvement reduces considerably between 5% and 7% content. A mathematical analysis of the parabolic function returns an optimum lime content near 6%. Similar behavior was obtained by Abbasi & Mahdih (2018). The dissolution of calcium hydroxide raises the pH of the mixture and allows the amorphous silica and alumina present in the pozzolanic material to combine with calcium to form hydrated compounds, in particular calcium silicate hydrate (Walker & Pavia, 2011; Sharma & Sivapullaiah, 2016). An increase in the lime content allows an optimization in the maintenance of this pH besides making more calcium ions available in the solution for the reactions to occur, however the low speed of the pozzolanic reaction and the reaching of an equilibrium pH can limit the strength gains.

An increase in relative density, as in the previous case, has a positive effect on the values of  $q_u$  and  $q_t$  for any lime content, meanwhile, the combined effect of relative density and lime content is less significant than the combined effect of relative density and PPW content. This can be attributed to the small difference between the lime contents studied, which has little impact on the amount of fines and hence on the granulometric characteristics of the mixtures.

As for the interaction between lime and PPW content the optimum region occurs at high values of PPW incorporation and lime contents between 5% and 7%. An increase in the amount of incorporated PPW requires greater amounts of calcium available for pozzolanic reactions, thus, mixtures with a high content of PPW and low amount of lime can limit strength gains by lack of calcium. In this case, part of the incorporated waste is dissolved and helps in the formation of the cementing compounds while other particles act only with a physical filling effect in the pores created by the larger sand particles (Moon et al., 2020).

It can be inferred that the optimization points for the response variables taking into account all three factors simultaneously have not yet been reached. The data indicate that these points are located at higher values of relative density and PPW content than those studied in this research. In other words, higher compressive and tensile strengths can be obtained for compacted samples with lime content between 5 and 7%, relative densities higher than 75%, and PPW contents above 30% simultaneously.

Figure 4 shows the variation of  $q_u$  and  $q_t$  with the volumetric binder content ( $B_{iv}$ ) for each relative density and lime content. Data predicted by Equations 13 and 14 were used. It can be noted that there is a tendency for the strength to increase with the increase of  $B_{iv}$ , with the slope of the curve being more pronounced for denser mixtures. Moreover, with the increase in relative density the behavior becomes more linear. An increase in the volume of binder incorporated enhances the cementation reactions, which is optimized by increasing the relative density, as discussed above. An important aspect is that the curves referring to the

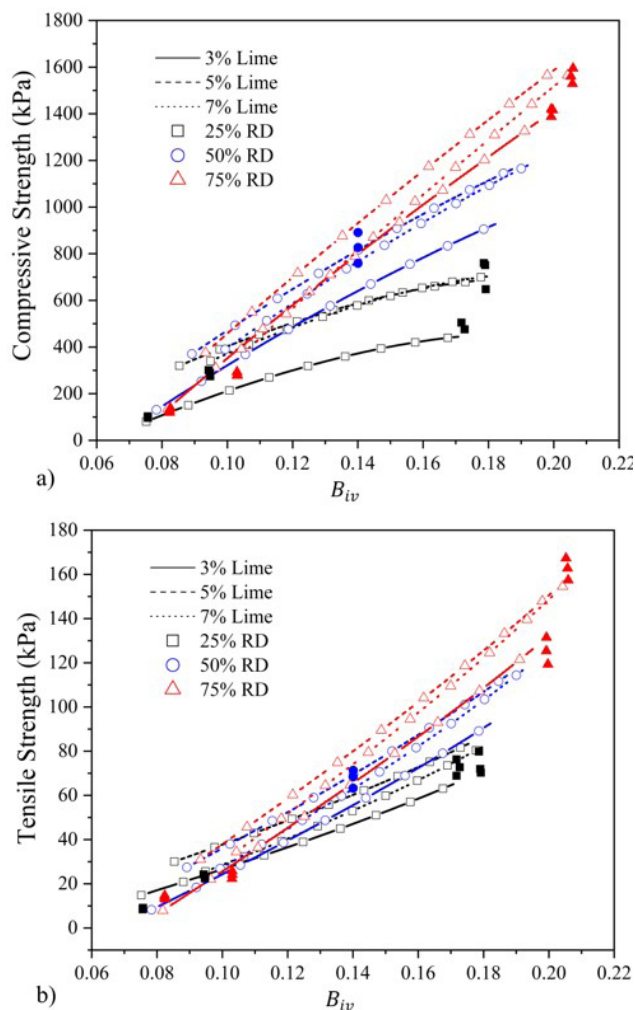


**Figure 4.** (a) Compressive and (b) Tensile strengths versus volumetric binder content.

7% lime content are located below those referring to the 5% content, i.e., for the same parameter  $B_{iv}$ , mixtures with 5% lime present higher strengths. Besides a better mechanical performance, this also indicates a better environmental performance of these mixtures since they require a smaller amount of lime and use larger volumes of waste.

Figure 5 illustrates the correlation of  $q_u$  and  $q_t$  with the parameter  $(\eta / B_{iv})$ . According to Consoli et al. (2016) the strength of soils treated with cementitious materials can be predicted by an equation such as Equation 15, where  $A$  is a scalar and  $B$  and  $\beta$  adjustment exponents. The values of  $B$  and  $\beta$  depend on the type of binder and the characteristics (particle size distribution and mineralogy) of the soil (Rios et al., 2013). The scalar  $A$ , according to Diambra et al. (2017), is related to the sand and binder matrix and is affected by the exponent  $B$ .

$$q_u = A \left[ \frac{\eta}{(B_{iv})^\beta} \right]^{-B} \quad (15)$$

In this paper a coefficient of determination  $R^2$  of 0.89 was obtained for the fitting curve. An exponent equal to 1.00 was applied to  $B_{iv}$ . Exponents smaller than 1.00 indicate that sample porosity has a greater effect on the mechanical strength of cemented soil. Values close to 1.00 indicate that the two parameters have similar effects and are most commonly used for the case of sandy soils (Baldovino et al., 2020a). Similar value was reported by Fontoura et al. (2021) who used the same soil as in this research. Mola-Abasi & Shooshpasha (2016) and Consoli et al. (2011, 2013, 2020b) obtained the same exponent for sands from other locations. However, the value of  $B$  equal to 2.30 differs from that reported in the other studies. According to Baldovino et al. (2020a) these parameters also depend on the compaction conditions, most often related to the optimum point obtained in the Proctor test.

In general, a reduction in  $\eta / B_{iv}$  leads to an increase in  $q_u$  and  $q_t$  with an exponential trend. Thus, a reduction in porosity combined with an increase in the amount of binder in the paste has a positive effect on the strength. Similar behavior was found by Baldovino et al. (2020b), Consoli et al. (2021) and Fontoura et al. (2021).

Another important aspect is that different mixture combinations can be obtained taking into account the same strength value. From Figure 5 it can be seen that the same strength can be obtained for different combinations of relative density, PPW content, and lime content. This indicates that although the parameter  $\eta / B_{iv}$  allows a good correlation of the data with the strength, a correct design of pozzolan-lime mixtures can only be made knowing the behavior of the strength in relation to the combinations between all the variables.

To be able to correlate the equations of the fit curves between  $q_t$  and  $q_u$  graphs, the  $q_t$  data was fitted to an equation with the same exponent  $B$  found for  $q_u$  (i.e., 2.30). It is worth mentioning that since it was the same soil, binder and preparation mode, these values were already close.

The ratio between  $q_t$  and  $q_u$  is shown in Equation 16. The value of 0.10 is a common value for the case of cemented materials (Khajeh et al., 2020; Consoli et al., 2020b). As shown in Table 5, the ratio between  $q_t$  and  $q_u$  for each mixture is also around 0.10.

$$\xi = \frac{q_t}{q_u} = \frac{802.7 \left( \frac{\eta}{B_{iv}} \right)^{-2.30}}{8020.6 \left( \frac{\eta}{B_{iv}} \right)^{-2.30}} = 0.10 \quad (16)$$

### 3.3 Effect of curing time on strength

Figure 6 shows  $q_u$  and  $q_t$  values of the FP-8 mixture (75% RD, 7% lime and 30% PPW) for 7, 28, and 91 days of curing. It is evident the strength improvement with the

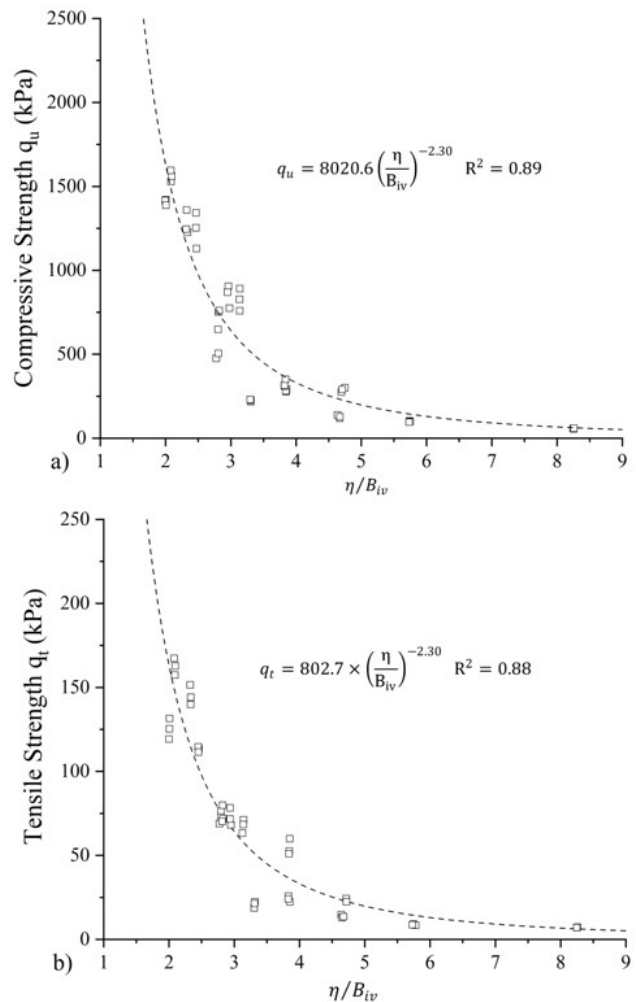


Figure 5. (a) Compressive and (b) Tensile strengths versus porosity/binder index.

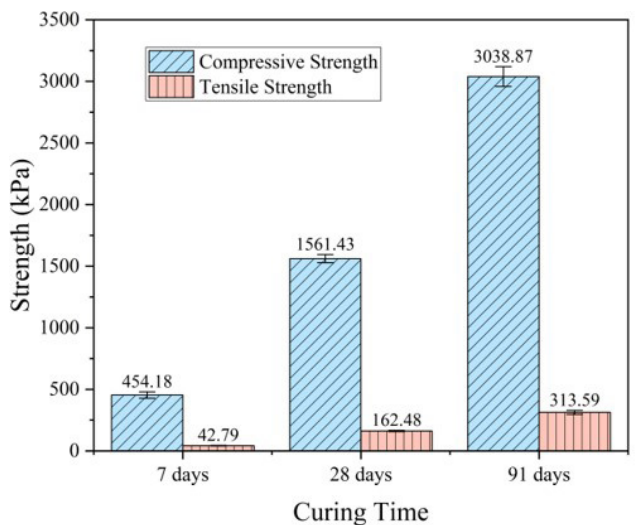


Figure 6. Variation of compressive and tensile strength with curing time.

increase of curing time. Values of  $q_u$  at 28 days and 91 days were, respectively, 243.7% and 569.1% higher than those found for 7 days. For  $q_t$  these increases were 279.7% and 632.9%. In addition, the ratio  $q_t / q_u$  is almost 0.1 for any of the curing times studied.

The increase in curing time allows the pozzolanic reactions, of low velocity, to occur, providing improvement in the bonding between the particles and increment in the mechanical performance of the soil (Consoli et al., 2001; Jha et al., 2009; Amadi & Osu, 2018; Khajeh et al., 2020). Increased strength with curing time was also obtained by Abbasi & Mahdih (2018) which evaluated the incorporation of a natural pozzolan and lime for the improvement of a sandy soil. Simatupang et al. (2020) also reported the increase of strength with curing time for sands stabilized with fly ash.

## 4. Conclusion

In this research, the influence of porcelain polishing waste and hydrated lime on the mechanical properties of an aeolian dune sand was investigated by unconfined compressive strength and split tensile strength tests. For this purpose, the variables relative density, lime content and PPW content were combined using a Surface Response Methodology with Central Composite Rotatable Design.

The PPW and lime contents as well as the relative density have a positive effect on  $q_u$  and  $q_t$  of the mixtures. The highest strength values were found for the region that combines high values of PPW content and relative density, being the optimum region above the one covered in this study. The influence of the lime content showed a parabolic behavior with the optimum content around 6%.

The improvement in the mechanical performance of the samples can be attributed to grain bonding due to cementation reactions. Pozzolanic reactions between lime and PPW and carbonation of lime are the most probable. At high PPW contents, the cementing compounds tend to be formed in the contact between the particles and an increment in the relative density and number of fines increases the number of contacts allowing higher strength gains.

It was possible to establish a good correlation of  $q_u$  and  $q_t$  data with the parameter  $\eta / B_{iv}$  and the strength is inversely proportional to this parameter. An exponent  $\beta$  equal to 1.00 was obtained indicating that porosity and volumetric binder content has similar effects. Finally, increases in  $q_u$  and  $q_t$  were obtained with increasing time of curing, demonstrating the dependence of cementation reactions to this factor in mixtures of soil, pozzolan and lime.

## Acknowledgements

The authors acknowledge the company Ceramics Elizabeth for supplying the porcelain polishing waste used in this research. The authors also thank the Coordination

for the Improvement of Higher Education (CAPES) and the National Council for Scientific and Technological Development (CNPQ) for the financial support granted for this research.

## Declaration of interest

The authors have no conflicts of interest to declare.

## Authors' contributions

José Daniel Jales Silva: conceptualization, data curation, methodology, formal analysis, investigation, writing – original draft, writing – review & editing. Olavo Francisco dos Santos Júnior: conceptualization, data curation, project administration, supervision, funding acquisition, writing – review & editing. William de Paiva: conceptualization, supervision, formal analysis, writing – review & editing.

## Data availability

The datasets generated analyzed in the course of the current study are available from the corresponding author upon request.

## List of symbols

$A$	Scalar for the relation between strength and $\eta / B_{iv}$
ANOVA	Analysis of variance
AP	Axial point
$B$	Second exponent of adjustment for the relation between strength and $\eta / B_{iv}$
$B_{iv}$	Volumetric binder content
$C_{iv}$	Volumetric cement content
$C_c$	Coefficient of curvature
$C_u$	Coefficient of uniformity
CCRD	Central composite rotatable design
CP	Central point
$d_{50}$	Mean diameter
$d_{10}$	Effective diameter
$df$	Degrees of freedom
$D$	Diameter of the sample
$e$	Void ratio
$e_{max}$	Maximum void ratio
$e_{min}$	Minimum void ratio
$F$	Maximum applied diametrical force
FP	Factorial point
$G_s$	Specific gravity
$H$	Height of the sample
$k$	Number of factors
$L$	Lime content
$M_d$	Total dry mass of the mixture
$M_{solids}$	Mass of solids
$M_S$	Mass of sand particles
$M_L$	Mass of lime particles

$M_p$	Mass of PPW particles
$M_w$	Mass of water
$MS$	Mean square
$n$	Number of experiments
$P$	PPW content
PPW	Porcelain polishing waste
$q_u$	Unconfined compressive strength
$q_t$	Split tensile strength
$R^2$	Coefficient of determination
RD	Relative density
$S$	Sand content
SP	Poorly graded sand
$SS$	Sum of squares
$V_{total}$	Total volume of the sample
$V_{solids}$	Volume of solids
$V_S$	Volume of sand particles
$V_L$	Volume of lime particles
$V_P$	Volume of PPW particles
$X_{(1,2,3)}$	Independent variables of polynomial equation
$Y$	Second order polynomial equation
$\beta$	First exponent of adjustment for the relation between strength and $\eta / B_{iv}$
$\beta_0$	Regression coefficient for intercept
$\beta_{(1,2,3)}$	Regression coefficients for linear behavior
$\beta_{(11,22,33)}$	Regression coefficients for quadratic behavior
$\beta_{(12,13,23)}$	Regression coefficients for interaction between factors
$\gamma_{d_{max}}$	Maximum dry unit weight
$\gamma_{d_{min}}$	Minimum dry unit weight
$\eta$	Porosity
$\eta / B_{iv}$	Porosity/binder index
$\xi$	Ratio between tensile strength and compressive strength
$\rho_d$	Dry density of the mixture
$\rho_S$	Density of sand particles
$\rho_L$	Density of lime particles
$\rho_P$	Density of PPW particles
$\rho_w$	Density of water

## References

- Abbasi, N., & Mahdieh, M. (2018). Improvement of geotechnical properties of silty sand soils using natural pozzolan and lime. *International Journal of Geo-Engineering*, 9(1), 1-12. <http://dx.doi.org/10.1186/s40703-018-0072-4>.
- ABNT NBR 12653. (2014). *Pozzolanic materials - Requirements*. ABNT - Associação Brasileira de Normas Técnicas, Rio de Janeiro, RJ (in Portuguese).
- ABNT NBR 5739. (2018). *Concrete - Compression test of cylindrical specimens*. ABNT - Associação Brasileira de Normas Técnicas, Rio de Janeiro, RJ (in Portuguese).
- ABNT NBR 7222. (2011). *Concrete and mortar - Determination of the tension strength by diametrical compression of cylindrical test specimens*. ABNT - Associação Brasileira de Normas Técnicas, Rio de Janeiro, RJ (in Portuguese).
- Åhnberg, H. (2006). *Strength of stabilised soil – a laboratory study on clays and organic soils stabilised with different types of binder* [Doctoral thesis, Lund University]. Lund University.
- Amadi, A.A., & Osu, A.S. (2018). Effect of curing time on strength development in black cotton soil–Quarry fines composite stabilized with cement kiln dust (CKD). *Journal of King Saud University-Engineering Sciences*, 30(4), 305-312. <http://dx.doi.org/10.1016/j.jksues.2016.04.001>.
- Andreola, F., Barbieri, L., Lancellotti, I., Bignozzi, M.C., & Sandrolini, F. (2010). New blended cement from polishing and glazing ceramic sludge. *International Journal of Applied Ceramic Technology*, 7(4), 546-555. <http://dx.doi.org/10.1111/j.1744-7402.2009.02368.x>.
- Andrew, R.M. (2018). Global CO<sub>2</sub> emissions from cement production. *Earth System Science Data*, 10(1), 195-217. <http://dx.doi.org/10.5194/essd-10-195-2018>.
- Anfacer, National Association of Ceramic Coating Manufacturers, Sanitary and Congeneral Suitcases. (2019). *Porfólio Anfacer 2019*. Retrieved in September 11, 2021, from <https://www.anfacer.org.br/setor-ceramico/numeros-do-setor>.
- ASTM C39-21. (2021). *Standard Test Method for Compressive Strength of Cylindrical Concrete Specimens*. ASTM International, West Conshohocken, PA. [https://doi.org/10.1520/C0039\\_C0039M-21](https://doi.org/10.1520/C0039_C0039M-21).
- ASTM C496-17. (2017). *Standard Test Method for Splitting Tensile Strength of Cylindrical Concrete Specimens*. ASTM International, West Conshohocken, PA. [https://doi.org/10.1520/C0496\\_C0496M-11](https://doi.org/10.1520/C0496_C0496M-11).
- Atkinson, A.C., & Donev, A.N. (1992). *Optimum experimental designs*. Oxford University Press.
- Baldovino, J.J.A., Izzo, R.L.S., da Silva, É.R., & Rose, J.L. (2020b). Sustainable use of recycled-glass powder in soil stabilization. *Journal of Materials in Civil Engineering*, 32(5), 04020080. [http://dx.doi.org/10.1061/\(ASCE\)MT.1943-5533.0003081](http://dx.doi.org/10.1061/(ASCE)MT.1943-5533.0003081).
- Baldovino, J.J.A., Izzo, R.L.S., Pereira, M.D., Rocha, E.V.G., Rose, J.L., & Bordignon, V.R. (2020a). Equations controlling tensile and compressive strength ratio of sedimentary soil–cement mixtures under optimal compaction conditions. *Journal of Materials in Civil Engineering*, 32(1), 04019320. [http://dx.doi.org/10.1061/\(ASCE\)MT.1943-5533.0002973](http://dx.doi.org/10.1061/(ASCE)MT.1943-5533.0002973).
- Bao, X., Jin, Z., Cui, H., Chen, X., & Xie, X. (2019). Soil liquefaction mitigation in geotechnical engineering: an overview of recently developed methods. *Soil Dynamics and Earthquake Engineering*, 120, 273-291. <http://dx.doi.org/10.1016/j.soildyn.2019.01.020>.
- Breitenbach, S.B. (2013). *Desenvolvimento de argamassa para restauração utilizando resíduo do polimento do porcelanato* [Master's dissertation, Universidade Federal

- do Rio Grande do Norte]. Universidade Federal do Rio Grande do Norte (in Portuguese).
- Bucci, M.G., Almond, P.C., Villamor, P., Tuttle, M.P., Stringer, M., Smith, C.M.S., Ries, W., Bourgeois, J., Loame, R., Howarth, J., & Watson, M. (2018). Controls on patterns of liquefaction in a coastal dune environment, Christchurch, New Zealand. *Sedimentary Geology*, 377, 17-33. <http://dx.doi.org/10.1016/j.sedgeo.2018.09.005>.
- Chang, T.S., & Woods, R.D. (1992). Effect of particle contact bond on shear modulus. *Journal of Geotechnical Engineering*, 118(8), 1216-1233. [http://dx.doi.org/10.1061/\(ASCE\)0733-9410\(1992\)118:8\(1216\)](http://dx.doi.org/10.1061/(ASCE)0733-9410(1992)118:8(1216)).
- Clough, G.W., Sitar, N., Bachus, R.C., & Shafii Rad, N. (1981). Cemented sands under static loading. *Journal of Geotechnical Engineering*, 107(6), 799-817. [http://dx.doi.org/10.1016/0148-9062\(81\)90544-1](http://dx.doi.org/10.1016/0148-9062(81)90544-1).
- Consoli, N.C., Bittar Marin, E.J., Quiñónez Samaniego, R.A., Heineck, K.S., & Johann, A.D.R. (2019b). Use of sustainable binders in soil stabilization. *Journal of Materials in Civil Engineering*, 31(2), 06018023. [http://dx.doi.org/10.1061/\(ASCE\)MT.1943-5533.0002571](http://dx.doi.org/10.1061/(ASCE)MT.1943-5533.0002571).
- Consoli, N.C., Carretta, M.S., Festugato, L., Leon, H.B., Tomasi, L.F., & Heineck, K.S. (2021). Ground waste glass-carbide lime as a sustainable binder stabilising three different silica sands. *Geotechnique*, 71(6), 480-493. <http://dx.doi.org/10.1680/jgeot.18.P.099>.
- Consoli, N.C., Cruz, R.C., & Floss, M.F. (2011). Variables controlling strength of artificially cemented sand: influence of curing time. *Journal of Materials in Civil Engineering*, 23(5), 692-696. [http://dx.doi.org/10.1061/\(ASCE\)MT.1943-5533.0000205](http://dx.doi.org/10.1061/(ASCE)MT.1943-5533.0000205).
- Consoli, N.C., da Silva, A., Barcelos, A.M., Festugato, L., & Favretto, F. (2020b). Porosity/cement index controlling flexural tensile strength of artificially cemented soils in Brazil. *Geotechnical and Geological Engineering*, 38(1), 713-722. <http://dx.doi.org/10.1007/s10706-019-01059-w>.
- Consoli, N.C., Ferreira, P.M.V., Tang, C.S., Marques, S.F.V., Festugato, L., & Corte, M.B. (2016). A unique relationship determining strength of silty/clayey soils-Portland cement mixes. *Soil and Foundation*, 56(6), 1082-1088. <http://dx.doi.org/10.1016/j.sandf.2016.11.011>.
- Consoli, N.C., Festugato, L., da Rocha, C.G., & Cruz, R.C. (2013). Key parameters for strength control of rammed sand-cement mixtures: influence of types of portland cement. *Construction & Building Materials*, 49, 591-597. <http://dx.doi.org/10.1016/j.conbuildmat.2013.08.062>.
- Consoli, N.C., Festugato, L., Scheuermann Filho, H.C., Miguel, G.D., Tebechrani Neto, A., & Andreghetto, D. (2020a). Durability assessment of soil-pozzolan-lime blends through ultrasonic-pulse velocity test. *Journal of Materials in Civil Engineering*, 32(8), 04020223. [http://dx.doi.org/10.1061/\(ASCE\)MT.1943-5533.0003298](http://dx.doi.org/10.1061/(ASCE)MT.1943-5533.0003298).
- Consoli, N.C., Leon, H.B., Carretta, M.S., Daronco, J.V.L., & Lourenço, D.E. (2019a). The effects of curing time and temperature on stiffness, strength and durability of sand-environment friendly binder blends. *Soil and Foundation*, 59(5), 1428-1439. <http://dx.doi.org/10.1016/j.sandf.2019.06.007>.
- Consoli, N.C., Prietto, P.D.M., Carraro, J.A.H., & Heineck, K.S. (2001). Behavior of compacted soil-fly ash-carbide lime mixtures. *Journal of Geotechnical and Geoenvironmental Engineering*, 127(9), 774-782. [http://dx.doi.org/10.1061/\(ASCE\)1090-0241\(2001\)127:9\(774\)](http://dx.doi.org/10.1061/(ASCE)1090-0241(2001)127:9(774)).
- Consoli, N.C., Winter, D., Leon, H.B., & Scheuermann Filho, H.C. (2018). Durability, strength, and stiffness of green stabilized sand. *Journal of Geotechnical and Geoenvironmental Engineering*, 144(9), 04018057. [http://dx.doi.org/10.1061/\(ASCE\)GT.1943-5606.0001928](http://dx.doi.org/10.1061/(ASCE)GT.1943-5606.0001928).
- Correia, A.A.S., Casaleiro, P.D.F., Figueiredo, D.T.R., Moura, M.S.M.R., & Rasteiro, M.G. (2021). Key-parameters in chemical stabilization of soils with multiwall carbon nanotubes. *Applied Sciences (Basel, Switzerland)*, 11(18), 8754. <http://dx.doi.org/10.3390/app11188754>.
- Correia, A.A.S., Lopes, L., & Reis, M.S. (2020). Advanced predictive modelling applied to the chemical stabilisation of soft soils. *Proc. of the Institution of Civil Engineers – Geotechnical Engineering*, (In Press) <http://dx.doi.org/10.1680/jgeen.19.00295>.
- Correia, A.A.S., Venda Oliveira, P.J., & Lemos, L.J.L. (2019). Strength assessment of chemically stabilised soft soils. *Proc. of the Institution of Civil Engineers – Geotechnical Engineering*, 172(3), 218-227. <http://dx.doi.org/10.1680/jgeen.17.00011>.
- De Matos, P.R., de Oliveira, A.L., Pelisser, F., & Prudêncio Junior, L.R. (2018a). Rheological behavior of Portland cement pastes and self-compacting concretes containing porcelain polishing residue. *Construction & Building Materials*, 175, 508-518. <http://dx.doi.org/10.1016/j.conbuildmat.2018.04.212>.
- De Matos, P.R., Jiao, D., Roberti, F., Pelisser, F., & Gleize, P.J. (2020). Rheological and hydration behaviour of cement pastes containing porcelain polishing residue and different water-reducing admixtures. *Construction & Building Materials*, 262, 120850. <http://dx.doi.org/10.1016/j.conbuildmat.2020.120850>.
- De Matos, P.R., Prudencio Junior, L.R., de Oliveira, A.L., Pelisser, F., & Gleize, P.J.P. (2018b). Use of porcelain polishing residue as a supplementary tabilizeds material in self-compacting concrete. *Construction & Building Materials*, 193, 623-630. <http://dx.doi.org/10.1016/j.conbuildmat.2018.10.228>.
- Diambra, A., Ibraim, E., Peccin, A., Consoli, N.C., & Festugato, L. (2017). Theoretical derivation of artificially cemented granular soil strength. *Journal of Geotechnical and Geoenvironmental Engineering*, 143(5), 04017003. [http://dx.doi.org/10.1061/\(ASCE\)GT.1943-5606.0001646](http://dx.doi.org/10.1061/(ASCE)GT.1943-5606.0001646).
- Elipe, M.G.M., & López-Querol, S. (2014). Aeolian sands: Characterization, options of improvement and possible employment in construction-The State-of-the-art.

- Construction & Building Materials*, 73, 728-739. <http://dx.doi.org/10.1016/j.conbuildmat.2014.10.008>.
- Fontoura, T.B., Santos Junior, O.F., Severo, R.N.F., Coutinho, R.Q., & Souza Junior, P.L. (2021). Unconfined compression strength of an artificially cemented aeolian dune sand of Natal/Brazil. *Soils and Rocks*, 44(1), e2021049920. <http://dx.doi.org/10.28927/SR.2021.049920>.
- German, R.M. (2014). Coordination number changes during powder densification. *Powder Technology*, 253, 368-376. <http://dx.doi.org/10.1016/j.powtec.2013.12.006>.
- Hoppe Filho, J., Gobbi, A., Pereira, E., Quarcioni, V.A., & Medeiros, M.H.F. (2017). Pozzolanic activity of mineral additions to Portland cement (Part I): pozzolanic activity index with lime (PAI), X-ray diffraction (XRD), thermogravimetry (TG/DTG) and modified Chapelle. *Matéria (Rio de Janeiro)*, 22(3), e11872. <https://doi.org/10.1590/S1517-707620170003.0206>
- Horpibulsuk, S., Miura, N., & Nagaraj, T.S. (2003). Assessment of strength development in cement-admixed high water content clays with Abrams' law as a basis. *Geotechnique*, 53(4), 439-444. <http://dx.doi.org/10.1680/geot.2003.53.4.439>.
- Jacoby, P.C., & Pelisser, F. (2015). Pozzolanic effect of porcelain polishing residue in Portland cement. *Journal of Cleaner Production*, 100, 84-88. <http://dx.doi.org/10.1016/j.jclepro.2015.03.096>.
- Jayanthi, P.N., & Singh, D.N. (2016). Utilization of sustainable materials for soil stabilization: state-of-the-art. *Advances in Civil Engineering Materials*, 5(1), 46-79. <http://dx.doi.org/10.1520/ACEM20150013>.
- Jha, J.N., Gill, K.S., & Choudhary, A.K. (2009). Effect of high fraction class F flyash on lime stabilization of soil. *International Journal of Geotechnics and Environment*, 1(2), 105-128.
- Khajeh, A., Chenari, R.J., & Payan, M. (2020). A simple review of cemented non-conventional materials: soil composites. *Geotechnical and Geological Engineering*, 38(2), 1019-1040. <http://dx.doi.org/10.1007/s10706-019-01090-x>.
- Latifi, N., Vahedifard, F., Ghazanfari, E., & Rashid, A.S.A. (2018). Sustainable usage of calcium carbide residue for stabilization of clays. *Journal of Materials in Civil Engineering*, 30(6), 04018099. [http://dx.doi.org/10.1061/\(ASCE\)MT.1943-5533.0002313](http://dx.doi.org/10.1061/(ASCE)MT.1943-5533.0002313).
- Li, L.G., Zhuo, Z.Y., Zhu, J., & Kwan, A.K.H. (2020). Adding ceramic polishing waste as paste substitute to improve sulphate and shrinkage resistances of mortar. *Powder Technology*, 362, 149-156. <http://dx.doi.org/10.1016/j.powtec.2019.11.117>.
- Li, L.G., Zhuo, Z.Y., Zhu, J., Chen, J.J., & Kwan, A.K.H. (2019). Reutilizing ceramic polishing waste as powder filler in mortar to reduce cement content by 33% and increase strength by 85%. *Powder Technology*, 355, 119-126. <http://dx.doi.org/10.1016/j.powtec.2019.07.043>.
- Mahvash, S., López-Querol, S., & Bahadori-Jahromi, A. (2018). Effect of fly ash on the bearing capacity of stabilized fine sand. *Proc. of the Institution of Civil Engineers - Ground Improvement*, 171(2), 82-95. <http://dx.doi.org/10.1680/jgrim.17.00036>.
- Medeiros, A.G., Gurgel, M.T., da Silva, W.G., de Oliveira, M.P., Ferreira, R.L., & de Lima, F.J. (2021). Evaluation of the mechanical and durability properties of eco-efficient concretes produced with porcelain polishing and scheelite wastes. *Construction & Building Materials*, 296, 123719. <http://dx.doi.org/10.1016/j.conbuildmat.2021.123719>.
- Mohamedzein, Y., Al-Hashmi, A., Al-Abri, A., & Al-Shereiqi, A. (2019). Polymers for stabilisation of Wahiba dune sands, Oman. *Proc. of the Institution of Civil Engineers - Ground Improvement*, 172(2), 76-84. <http://dx.doi.org/10.1680/jgrim.17.00063>.
- Mola-Abasi, H., & Shooshpasha, I. (2016). Influence of zeolite and cement additions on mechanical behavior of sandy soil. *Journal of Rock Mechanics and Geotechnical Engineering*, 8(5), 746-752. <http://dx.doi.org/10.1016/j.jrmge.2016.01.008>.
- Moon, S.W., Vinoth, G., Subramanian, S., Kim, J., & Ku, T. (2020). Effect of fine particles on strength and stiffness of cement treated sand. *Granular Matter*, 22(1), 1-13. <http://dx.doi.org/10.1007/s10035-019-0975-6>.
- Ribeiro, D., Néri, R., & Cardoso, R. (2016). Influence of water content in the UCS of soil-cement mixtures for different cement dosages. *Procedia Engineering*, 143, 59-66. <http://dx.doi.org/10.1016/j.proeng.2016.06.008>.
- Rios, S., Fonseca, A.V., & Baudet, B.A. (2014). On the shearing behaviour of an artificially cemented soil. *Acta Geotechnica*, 9(2), 215-226. <http://dx.doi.org/10.1007/s11440-013-0242-7>.
- Rios, S., Fonseca, A.V., Consoli, N.C., Floss, M., & Cristelo, N. (2013). Influence of grain size and mineralogy on the porosity/cement ratio. *Géotechnique Letters*, 3(3), 130-136. <http://dx.doi.org/10.1680/geolett.13.00003>.
- Rogers, C.D.F., Glendinning, S., & Roff, T.E.J. (1997). Lime modification of clay soils for construction expediency. *Proc. of the Institution of Civil Engineers - Geotechnical Engineering*, 125(4), 242-249. <http://dx.doi.org/10.1680/igeng.1997.29660>.
- Sánchez de Rojas, M.I., Frías, M., Sabador, E., Asensio, E., Rivera, J., & Medina, C. (2018). Use of ceramic industry milling and glazing waste as an active addition in cement. *Journal of the American Ceramic Society*, 101(5), 2028-2037. <http://dx.doi.org/10.1111/jace.15355>.
- Saxena, S.K., & Lastrico, R.M. (1978). Static properties of lightly cemented sand. *Journal of the Geotechnical Engineering Division*, 104(12), 1449-1465. <http://dx.doi.org/10.1061/AJGEB6.0000728>.
- Schnaid, F., Prietto, P.D.M., & Consoli, N.C. (2001). Characterization of cemented sand in triaxial compression. *Journal of Geotechnical and Geoenvironmental Engineering*,

- 127(10), 857-868. [http://dx.doi.org/10.1061/\(ASCE\)1090-0241\(2001\)127:10\(857\)](http://dx.doi.org/10.1061/(ASCE)1090-0241(2001)127:10(857)).
- Sharma, A.K., & Sivapullaiah, P.V. (2016). Strength development in fly ash and slag mixtures with lime. *Proc. of the Institution of Civil Engineers - Ground Improvement*, 169(3), 194-205. <http://dx.doi.org/10.1680/jgrim.14.00024>.
- Sharma, M., Satyam, N., & Reddy, K.R. (2021). State of the art review of emerging and biogeotechnical methods for liquefaction mitigation in sands. *Journal of Hazardous, Toxic and Radioactive Waste*, 25(1), 03120002. [http://dx.doi.org/10.1061/\(ASCE\)HZ.2153-5515.0000557](http://dx.doi.org/10.1061/(ASCE)HZ.2153-5515.0000557).
- Silvani, C., Benetti, M., & Consoli, N.C. (2019). Maximum tensile strength of sand-coal fly ash-lime blends for varying curing period and temperature. *Soils and Rocks*, 42(1), 83-89. <http://dx.doi.org/10.28927/SR.421083>.
- Simatupang, M., Mangalla, L.K., Edwin, R.S., Putra, A.A., Azikin, M.T., Aswad, N.H., & Mustika, W. (2020). The mechanical properties of fly-ash-stabilized sands. *Geosciences*, 10(4), 132. <http://dx.doi.org/10.3390/geosciences10040132>.
- Souza Júnior, P.L., Santos Junior, O.F., Fontoura, T.B., & Freitas Neto, O. (2020). Drained and undrained behavior of an aeolian sand from Natal, Brazil. *Soils and Rocks*, 43(2), 263-270. <http://dx.doi.org/10.28927/SR.432263>.
- Venda Oliveira, P.J., & Cabral, D.J.R. (2021). Behaviour of a silty sand stabilized with xanthan gum under unconfined and confined conditions. *Proceedings of the Institution of Civil Engineers - Ground Improvement* (In press) <http://dx.doi.org/10.1680/jgrim.20.00065>.
- Venda Oliveira, P.J., & Rosa, J.A.O. (2020). Confined and unconfined behavior of a silty sand improved by the enzymatic biocementation method. *Transportation Geotechnics*, 24, 100400. <http://dx.doi.org/10.1016/j.trgeo.2020.100400>.
- Venda Oliveira, P.J., Costa, M.S., Costa, J.N.P., & Nobre, M.F. (2015). Comparison of the ability of two bacteria to improve the behaviour of a sandy soil. *Journal of Materials in Civil Engineering*, 27(1), 06014025. [http://dx.doi.org/10.1061/\(ASCE\)MT.1943-5533.0001138](http://dx.doi.org/10.1061/(ASCE)MT.1943-5533.0001138).
- Vranna, A., & Tika, T. (2020). Undrained monotonic and cyclic response of weakly cemented sand. *Journal of Geotechnical and Geoenvironmental Engineering*, 146(5), 04020018. [http://dx.doi.org/10.1061/\(ASCE\)GT.1943-5606.0002246](http://dx.doi.org/10.1061/(ASCE)GT.1943-5606.0002246).
- Vranna, A., & Tika, T. (2021). Laboratory improvement of liquefiable sand by colloidal silica and weak cementation. *Proceedings of the Institution of Civil Engineers - Ground Improvement*, 174(4), 240-251.
- Walker, R., & Pavía, S. (2011). Physical properties and reactivity of pozzolans, and their influence on the properties of lime–pozzolan pastes. *Materials and Structures*, 44(6), 1139-1150. <http://dx.doi.org/10.1617/s11527-010-9689-2>.
- Wiącek, J., & Molenda, M. (2014). Effect of particle size distribution on micro-and macromechanical response of granular packings under compression. *International Journal of Solids and Structures*, 51(25-26), 4189-4195. <http://dx.doi.org/10.1016/j.ijsolstr.2014.06.029>.
- Zhang, R.J., Santoso, A.M., Tan, T.S., & Phoon, K.K. (2013). Strength of high water-content marine clay stabilized by low amount of cement. *Journal of Geotechnical and Geoenvironmental Engineering*, 139(12), 2170-2181. [http://dx.doi.org/10.1061/\(ASCE\)GT.1943-5606.0000951](http://dx.doi.org/10.1061/(ASCE)GT.1943-5606.0000951).